



# Land use/land cover change impact on streamflow using Arc-SWAT model, in case of Fetam watershed, Abbay Basin, Ethiopia

Yitbarek Andualem Mekonnen<sup>1</sup> · Temesgen Mekuriaw Manderso<sup>1</sup>

Received: 11 November 2022 / Accepted: 28 March 2023 / Published online: 10 April 2023  
© The Author(s) 2023

## Abstract

Changes in Land Use Land Cover (LULC) are currently one of the greatest pressing issues facing the watershed, its hydrological properties of soil, and water management in catchment areas. One of the most important elements impacting streamflow in watersheds is LULC change. The main objective of this study was to evaluate the effect and future predication of LULC change on streamflow of the Fetam watershed by using Cellular Automata (CA)-Markov in IDRISI software. To analyze the impact of land use/cover change on streamflow, the Soil and Water Assessment Tool (SWAT) calibration and validation model was used. LULC map was developed by using Cellular Automata (CA)-Markov in IDRISI software, and the coverage of LULCs was including parameters of cropland, vegetation, grassland, Built-up area/Urban and water body. The findings of this study showed that the major challenges of land use/cove changes were rapid population increase, farming, and industrial activity. During the study period (2000–2020), most portions of the water body, vegetation, and grassland were changed into cropland and constructed by building. Cropland and construction areas increased by 15% and 46.95%, respectively, whereas water bodies, vegetation, and grassland decreased by 62.7%, 70.02%, and 38.1%, respectively. According to the forecasted results for the period of 2030–2040, cropland and built-up areas are increased, while vegetation, grassland, and water bodies were decreased. The SWAT model's calibration and validation performance was evaluated using the streamflow of the most sensitive parameters. For the years 2000–2004, and 2005–2012, the models were calibrated and validated, and the results showed good agreement between observed and simulated streamflow, with NSE and  $R^2$  values of 0.88 and 0.72 and 0.9 and 0.85, respectively. The results of this study indicated that the seasonal streamflow was decreased from 2000 to 2010 and 2010–2020 years during the dry and rainy seasons. In general, the impacts of land use/cover change on streamflow are significant considerations for planning and implementing water resource projects. In order to address the risks, effective land-use planning and climate-resilient water management strategies will be improved.

**Keywords** LULC change · SWAT · Streamflow · ERDAS · Fetam watershed

## Introduction

The availability and competition for water will vary as a result of land use/land cover change (LULCC) and climate change, which are brought on by regional and global economic development (Dibaba et al. 2020; Disse et al. 2018; Mekonnen et al. 2022). High rainfall variability, rising food and water needs, frequent hydrological extremes, and rapid

population growth all contribute to the environment's continued degradation by affecting the availability of various biophysical resources. In addition, to satisfy the demands of an expanding population, agricultural land expansion and intensification, urban area growth, and the requirement to extract wood products and fire fuel are all on the rise (Gashaw et al. 2018; Woldesenbet et al. 2018). Since LULCC is not only a local environmental problem but is also growing into a force of global significance, it will have an impact on important parts of how the earth's system functions when it aggregates globally (Disse et al. 2018). There is a chance that climate change will put further strain on the accessibility and availability of water. Interest in how these changes will affect the hydrological process will grow as a result of the projected negative environmental implications of these

✉ Yitbarek Andualem Mekonnen  
yitbarekandu12@gmail.com

Temesgen Mekuriaw Manderso  
tmekuriaw1485@gmail.com

<sup>1</sup> Department of Hydraulic and Water Resources Engineering,  
Debre Tabor University, Debre Tabor, Ethiopia

changes (Alemu et al. 2022; Dibaba et al. 2020; Mekonnen et al. 2022). The demand for fresh water is correlated with changes in lifestyle, economic growth, and population size. Water scarcity is a result of both excessive human demand and hydrological unpredictability (Alemu et al. 2022). Natural resources include land, water, air, energy sources, plants, soil, animals, and minerals, all of which are derived from nature. These resources are critical components of a catchment's of environment, providing socio-economic and ecological benefits to society (Chen et al. 2020; Hassaballah et al. 2017; Kidane et al. 2019; Tena et al. 2019; Yihun 2020).

The change in land use/cover in a given area is a result of environmental and socioeconomic issues, as well as human activity over time and space. Increases and decreases in population growth in the system, climate, financial development, and physical elements such as landscape, grade condition, and soil type all have an impact on Land Uses land Cover (LULC) changes (Mekonnen et al. 2022; Moges et al. 2017; Tewabe and Fentahun 2020).

Land use and land cover change is a major issue when discussing universal dynamics and how they respond to hydrologic features of water and soil administration in a catchment (Chang et al. 2018; Welde and Gebremariam 2017). Land cover/use and climate change has a important effect on the watershed's hydrological processes. The consequences of land use/land cover and climate change are predicted to increase in the future as a result of growing forest area clearing for farming and rising global temperatures (Hu et al. 2019; Hyandye et al. 2018). Increased deforestation, suburbanization, agriculture, and everyday actions of human-caused time-based and spatial changes in land use/cover, which have influenced flow aquatic path patterns and aquatic stability (Bufebo and Elias 2020; Welde and Gebremariam 2017).

The technique in which the land has been put to use (land use/land cover) is defined, with a focus on the land's useful function in financial events. However, land-cover refers to the physical characteristics of the earth's surface, which are distributed in the form of vegetation, water, soil, and other physical characteristics of the land, including those created entirely by human activities such as continuous cultivation, deforestation, and overgrazing (Bekele 2019; Bufebo and Elias 2020; Saddique et al. 2020).

In Ethiopia, where 85% of the population works in agriculture and is dependent on current water supplies, analyzing and administering existing water resources is a big issue. The surface and rainwater flow model is a useful tool for investigating surface and rainwater systems and administering watersheds (Anmut et al. 2020; Bogale 2020).

Increased population and the constant demand for large amounts of food are the primary factors in Ethiopia, causing natural forests to be converted to urbanization, grasslands, and agricultural lands. As a result, they are the primary contributors to changes in land use and cover (Fentie et al. 2020; Tewabe and Fentahun 2020). The most common variations in land use/cover in our country include the changing of natural forests to farming lands, urban areas, overgrazing land, and other industrial and institutional areas (Fentie et al. 2020; Hyandye et al. 2018; Yohannes et al. 2018). As a consequence, agronomic fields have been enlarged at the expenditure of natural forests in order to deal with infrequent nutrition shortages for growing communities (Abere et al. 2020; Hyandye et al. 2018; Saddique et al. 2020). As a consequence, the landscapes of numerous watersheds must be enhanced, and the extent of the watershed has been increased to create good environments (Fentie et al. 2020; Yohannes et al. 2018).

Streamflow is a critical hydrological variable for water source preparation, design, and advance; this hydrological action is inextricably linked to LULC (Anmut et al. 2020; Bogale 2020). The tendency of overgrazing, farming and deforestation in the Fetam watershed has been expanding from time to time, due to the increase in farming land, which causes the land use/cover change of the catchment spaces. This constant land use/cover shift has changed the water stability of the catchment through altering the quantity and shapes of the mechanisms of streamflow, which include groundwater flow, surface runoff, and lateral flow. These effects have increased the degrees of water management challenges in study areas (Chen et al. 2020; Chimdessa et al. 2019; Mekonnen et al. 2022).

Changes in land use/cover have an impact on evapotranspiration, infiltration, erosion, and an interception in the runoff process (Abidin et al. 2017; Dibaba et al. 2020; Tena et al. 2019). In the current hydrological scenario, this causes a deal of issues. Land use/cover change is a type of increasing the percentage of the waterproof layer, which increases the amount of surface runoff and decreases the amount of water infiltrated into the ground. It also reduces the time of concentration, which causes many interruptions by producing higher volumes of runoff and lowering the amount of water infiltrated into the ground. These and other issues must be thoroughly examined in order to determine the effects of land use on various hydrological procedures in the research area (Bekele 2019; Bufebo and Elias 2020; Hasan et al. 2020; Owar Othow et al. 2017).

At this time, the study area is rapidly developing by infrastructures, such as rapid population growth with no gaps, urbanization, institutional and industrial facilities, increasing agricultural land, and requiring huge amounts of food

production, all of which affect land use, land cover, and streamflow changes. The Fetam river watershed, landscape quantification, and economic production of the research area, as well as the country, are all affected by LULC change in some way. The Fetam watershed is one of the most important natural resources; it faces numerous issues as a result of urbanization, population growth, agricultural land, and industrialization, all of which contribute to rapid changes in land use/cover, and land degradation in the Fetam River. Land degradation is defined as the loss of top-fertilized soil due to flooding during the rainy season and a reduction in water supply for irrigation during the dry season; this is the most common concern in the Fetam watershed's streamflow. This study has been started specifically to examine into the watershed's hydrological reaction to the LULC change. LULC prediction was using integrated CA-Markov analytic methods. The evaluation of the isolated and combined LULC change was conducted using the hydrological modeling component of the Soil and Water Assessment Tool (SWAT). The major goal of this study was to determine the impact and future predication of land use and land cover change on streamflow in the Fetam watershed in Ethiopia's upper Blue Nile basin from 2000 to 2020 by using Cellular Automata (CA)-Markov in IDRISI software.

## Methods and materials

### Description of the investigation area

The Fetam basin is one of the southern Upper Blue Nile basins. In the southern Upper Blue Nile basins, the catchment is located between 10o20'51.43" N and 11o01'23.4" N latitude and 37o52'02.02" E and 36o55'2.56" E longitude (Fig. 1). Fetam Rivers drain Awi Zone Banja, Injibara, Guagusa shikudad wordas and West Gojjam Zone Sekella, Bure Zuria, Bure Ketema, Womberima Woredas in Amhara National Regional State, 432 km north of Addis Ababa. The study area's watershed was estimated to be 757.53 km<sup>2</sup> (Fig. 1).

### Climate of Fetam watershed

The year is divided into two seasons based on rainfall patterns: dry and rainy periods. The dry period started from November to April, while the wet period started from June to September. May and October are transitional months with frequent light rainfall. Through the wet period of June to September, the study area receives 70–90% of its yearly

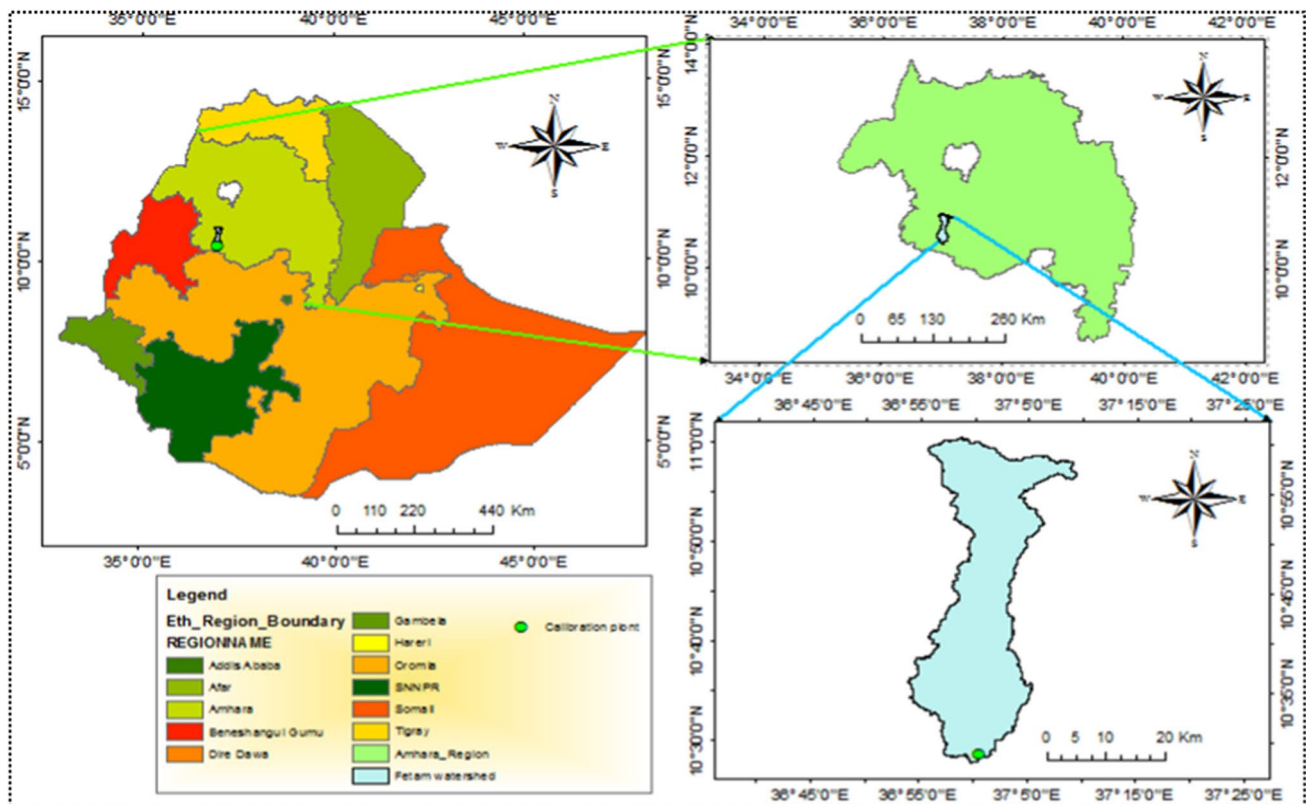


Fig. 1 Location of Fetam catchment (Source: Ministry of Water resources)

precipitation. The research area's mean yearly precipitation is 1896.97 mm, but there is a minor spatial variance within the area. The study area's monthly temperatures fluctuate from month to month, ranging from 9.1 to 29.9 °C. The monthly mean extreme temperature ranges from 23.8 °C in July to 31.1 °C in March, while the monthly mean minimum temperature ranges from 9.9 degrees Celsius in January and December to 14.2 degrees Celsius in May. March and April are the months with the greatest average temperatures. The monthly maximum temperature and monthly mean rainfall of five watershed stations are given in the graph below (Fig. 2).

## Methods and data collection

Methods of this study are mainly focusing on assessing the impacts of land use/cover changes on stream flow of Fetam watershed by using Acr-SWAT model and collect the most important data.

### SWAT model input data

Landsat imagery from the United States Geological Survey (USGS) commencing in 2000, 2010, and 2020, as well as a shapefile of the Fetam River basin, were used in this study. These data included a DEM with a resolution of 30 m by 30 m, soil types, meteorological, hydrological, and flow data, as well as land use and land cover data.

### Soil data

Soil data are one of the main inputs for the SWAT model (Gashaw et al. 2020). The soil map for this study area was provided by Ethiopia's Ministry of Water, Irrigation, and Energy. The Fetam watershed highland is a flat plain watershed dominated by Nitisol and Vertisol, both of which have a main textural class of sandy clay and sandy loam. However, the predominant soil types found in the watershed's hills and lowlands are shallow Leptisols and cambisols.

The Fetam watershed is divided into five main soil classes according to FAO categorization. These are Cambisols, Leptisols, Luvisols, Nitisols, and Vertisols (Fig. 3). For distinct layers of each soil type, the SWAT model needed physical and chemical parameters such as organic carbon content, hydraulic conductivity, soil texture, available water content, and bulk density, some of which will be taken from the Harmonized World Soil Database (HWSD) (Roy and Inamdar 2019).

### Hydrological data

Hydrological data, which includes daily streamflow or water discharge data from 2000 to 2020, are collected from the MoWIE's Hydrology Department. These data were used to calibration and validation models of hydrological components. Hydrological data are used to predict the effect of land administration methods such as reservoir administration, land use/cover changes, groundwater withdrawals, and water transmissions in complicated watersheds (Fentie et al. 2020). The model predicts important hydrological variables such as surface stormwater, maximum runoff, evapotranspiration, sediment output, and groundwater inflows for each HRUs unit.

### Meteorological data

To simulate the river's hydrological circumstances, the SWAT model required climatological data. The National Meteorological Agency of Ethiopia provided the climatological data required for this investigation, which could be read from a measured data set using a weather generator model. Minimum and Maximum temperatures, rainfall, wind speed, comparative humidity, and sunlight are all essential climatological data, but rainfall was the most important one for this study, which covered four sites from 2000 to 2020. Injibara, Sekela, Tilil, Bure, and Shindi are the stations that are located in and near the study area, shown in (Fig. 4). The missing data are given a value of -99, which is filled

**Fig. 2** Monthly temperatures of five stations around Fetam River

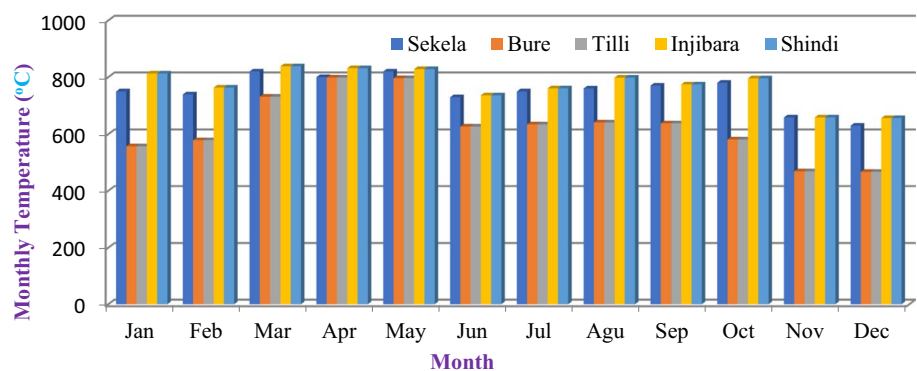
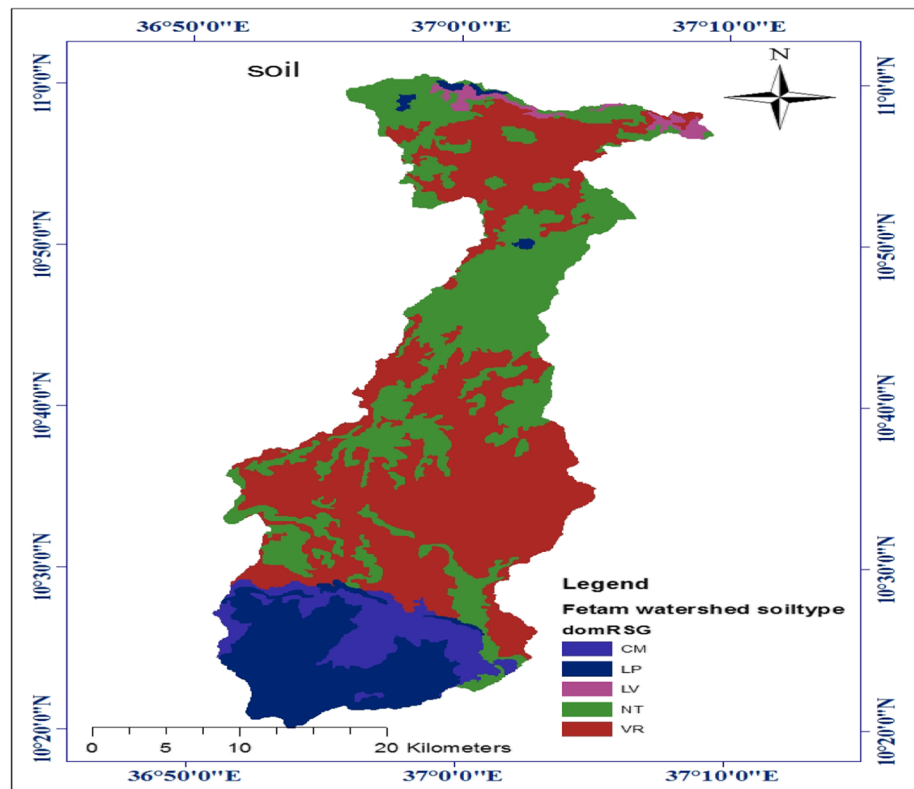


**Fig. 3** Soil map of Fetam Watersheds (ministry of water resources)



by weather generators and prepared for input into the SWAT model.

#### Land use/covers data

Another major factor influencing evapotranspiration, runoff, and surface degradation in a watershed is LULC changes. The Fetam watershed land uses/cover changes from time to time due to various issues primarily changing by urbanization, agricultural practice, and irrigation expansion. Before the analysis can begin, LULC change studies frequently necessitate the increase in land cover components. The Landsat data image of the watershed which displays the land use land cover for three different years of 2000, 2010, and 2020 were downloaded from satellite images downloaded from USGS-GLOVIS ([www.glovis.usgs.gov](http://www.glovis.usgs.gov)) used for land use change detection of the study area.

#### Methods of data analysis

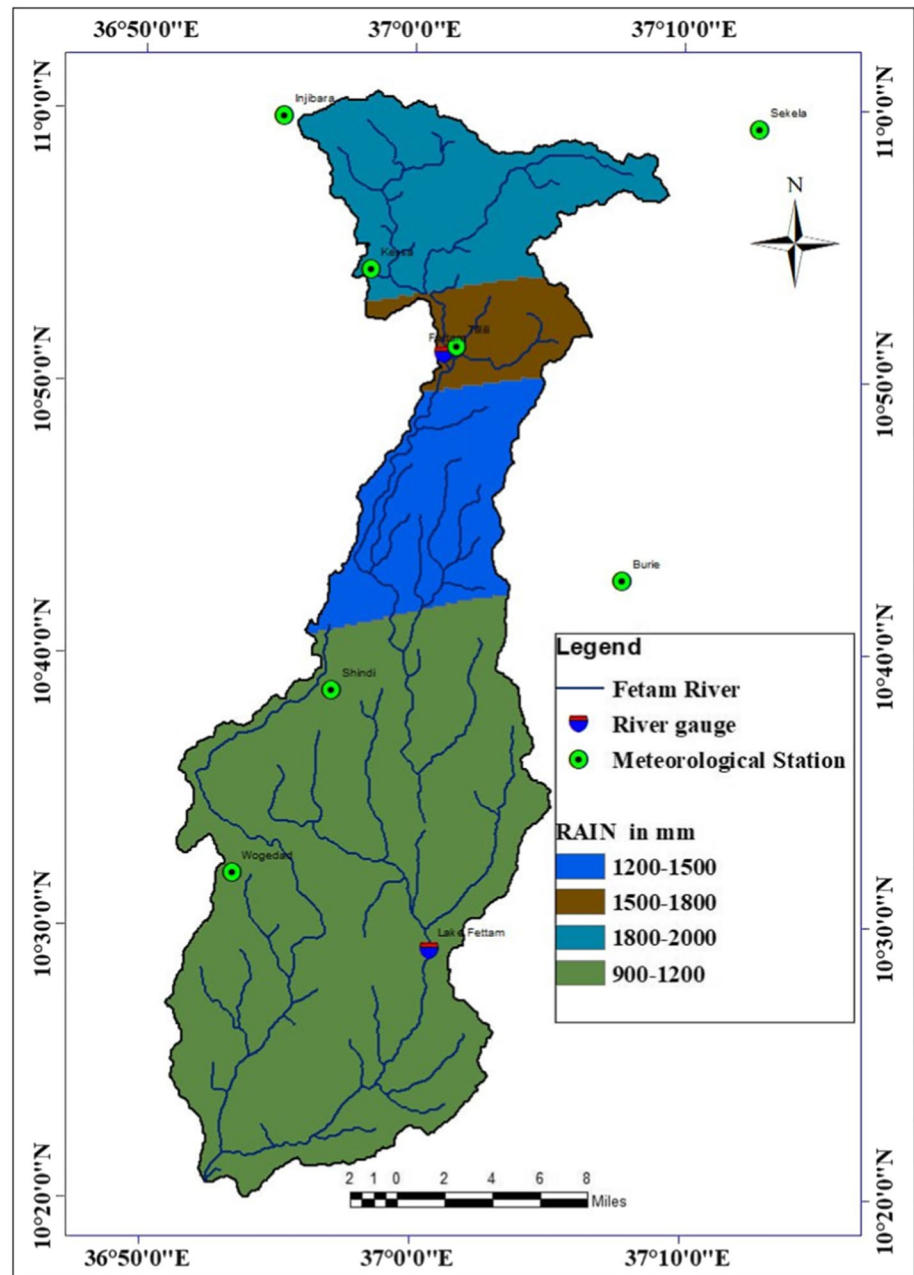
##### Land use land cover analysis

**Image pre-processing and processing** The aim of this investigation was to determine changes in LULC delivery in the Fetam watershed during a 20-year period from 2000 to 2020 using Land sat imageries from three groups. For the years 2000–2020, the land sat ETM+ was chosen. Layer

stacking is performed on 7 images for landsat5, 8 images for land sat7, and 11 images for land sat8 before being composited into three groups (3, 2, 1) for Land sat 7 and Land sat 5, and a single layer for Land sat 8 (4, 3, 2). To reduce the seasonal change in forest shape and delivery through the year, the developed statistics dates are chosen as closely as likely in the similar yearly period of the developed years. All of the input satellite photos are false-color produced to distinguish and depict the surface landscapes clearly; these images cover the whole Fetam watershed.

**LULC classification** This study employed digital image classification to determine land use and cover. The technique of arranging all of the input images into a small number of data classes was well-defined in digital image classification. The CA-Markov model combines the benefits of CA theory with the Markov model's capacity for temporal forecasting. As a result, the CA-Markov model performs better than the other techniques for simulating the temporal and spatial aspects of LULC changes (Yang et al. 2019). Two techniques Markov chain analysis and CA are used in the CA-Markov approach in IDRISI. In this investigation, the methods for projecting LULCCs with CA-Markov described by Pan et al. (2017) were applied within the IDRISI software framework. Creating suitability maps, calculating the transition matrix, and predicting the LULC map are the three steps of the procedure. The Markov chain model in IDRISI developed the LULC transi-

**Fig. 4** The location of meteorological and hydrological gauge and rainfall distribution systems



tion matrix. Then, using a multi-criteria evaluation (MCE), the suitability maps of the probable driving elements of the LULC translations are developed for each LULC class. To create suitability maps, parameters including cropland, vegetation, grassland, Built-up area/Urban and water body were taken into consideration. Finally, the suitability maps and transition matrix are used to predict the LULC maps. Three LULC maps were developed for the LULCC study for the years 2000, 2010, and 2020. Future land use maps of LULC2030 and LULC2040 were predicted using the CA-Markov algorithm in the IDRISI software using the land use maps of 2010 and 2020 as a baseline. Model calibration and validation are

essential for every model prediction. The model's validation outcomes will then determine how useful the model output is. Kappa coefficients derived from Eq. (1) were used to evaluate the CA-Markov model's efficacy in predicting land use maps (Dibaba et al. 2020; Pan et al. 2017). In this study, the 2020 LULC map was simulated using the LULC maps from 2000 and 2020. Then, using the Kappa index, the observed 2020 LULC map was contrasted with the simulated 2020 LULC map.

$$\text{Kappa} = \frac{P_O - P_C}{1 - P_C} \quad (1)$$

where  $P_o$  is the percentage of accurately simulated cells in the equation above, and  $P_c$  is the anticipated proportional error due to chance between the observed and simulated map. If  $Kappa \leq 0.5$  indicates sparse agreement,  $0.5 \leq Kappa \leq 0.75$  indicates moderate agreement,  $0.75 \leq Kappa \leq 1$  indicates great agreement, and  $Kappa = 1$  indicates complete agreement.

During the accuracy test of image classification of the years 2000 and 2010, GIS software was used to change the regulator points collected from Google Earth to shapefile, but 2020 collocate on the field. The following diagrams show the classification of land use/cover (Table 1).

**Meteorological data analysis**

**Filling of missing data** Data from a certain gauge station are unavailable, or illustrative precipitation is required at interest points. Using the average and normal ratio approach to use the rainfall in this study area, there are several procedures to fill in the missing data from that station. Initiate, calculate the percentage difference, to calculate the filling missing data at necessary station using this equation:

$$P_x = \frac{\sum_{i=1}^N \frac{P_i}{d_i^2}}{\sum_{i=1}^N \frac{1}{d_i^2}} \tag{2}$$

where  $P_x$  is A real average rainfall;  $P_i$  is Rainfall measured at station ‘i’;  $d_i$  is the distance of sub-region for places ‘i’;  $n$  is the numeral of neighboring locations.

**Table 1** Land use/covers classification of study area

No	Major units	Sub units within the major units
1	Cropland/agriculture	Intensively cultivated land Moderately cultivated land Scattered cultivated land within shrubs
2	Vegetation/forest	Dense natural forest Plantation forest Natural and plantation forest
3	Grass land	Wooded grass land Open grass land Shrub grass land Open shrub land Dance bush land Degraded wooded shrub land
4	Built-up area/urban	Villages Roads Town
5	Water	Water pond River Reservoir

Other missing meteorological data, such as temperature, relative humidity, wind speed, and sunlight hour, were given – 99 values and prepared for SWAT input by weather generators (Gashaw et al. 2020; Chen et al. 2020; Tenagashaw et al. 2022).

**Homogeneity and trend test** Time series homogeneity tests allow for the identification of a change as well as a time series. It is used to determine whether a series is homogeneous across time. Rainfall records at gauging stations are influenced by the station’s location, the tool, and the method used to record and collect data, as well as the observation quality, and the time series may be inhomogeneous. As a result, the data utilized in the modeling of water resources and hydrology procedures would be statistically evaluated for reliability and quality. Rainbow and non-dimensional charts are commonly used to verify the homogeneity of rainfall time series data. As a consequence, while selecting an illustrative meteorological location for the research of areal precipitation approximation, examining the homogeneity of group stations is crucial. The similarity of the selecting gauging locations’ monthly rainfall records was computed using the non-dimensional plot method. The following equation is used to test the homogeneity and trend of the average annual rainfall of all stations in and around the Fetam watershed from 2000 to 2020.

$$P_i = \frac{P_{i.av}}{P_{av}} * 100 \tag{3}$$

where  $P_{i.av}$  is the over year’s average monthly precipitation for the place I and  $P_{ave}$  is the over year’s average yearly precipitation for the site  $i$ . Because the meteorological and hydrological data are homogeneous. The homogeneity and trend test of rainfall data in five metrological places are shown in Fig. 5.

**Checking the consistency of data**

A continuous recording is one in which the qualities of the data in the record are retained over the period. To correct for measure consistency, the calculation of a result is employed rather than a missing value. Changes in the monitoring process, changes in the gauge’s station, and changes in land use may necessitate modification when maintaining the gauge at its original site is impractical, and when damage occurs regularly. For adjusted inconsistency data, the approach of double mass-curve analysis was employed to validate the consistency of precipitation in a gauge record. Equation 4 should be used to correct it.

$$P'X = P_x \frac{M'}{M} \tag{4}$$

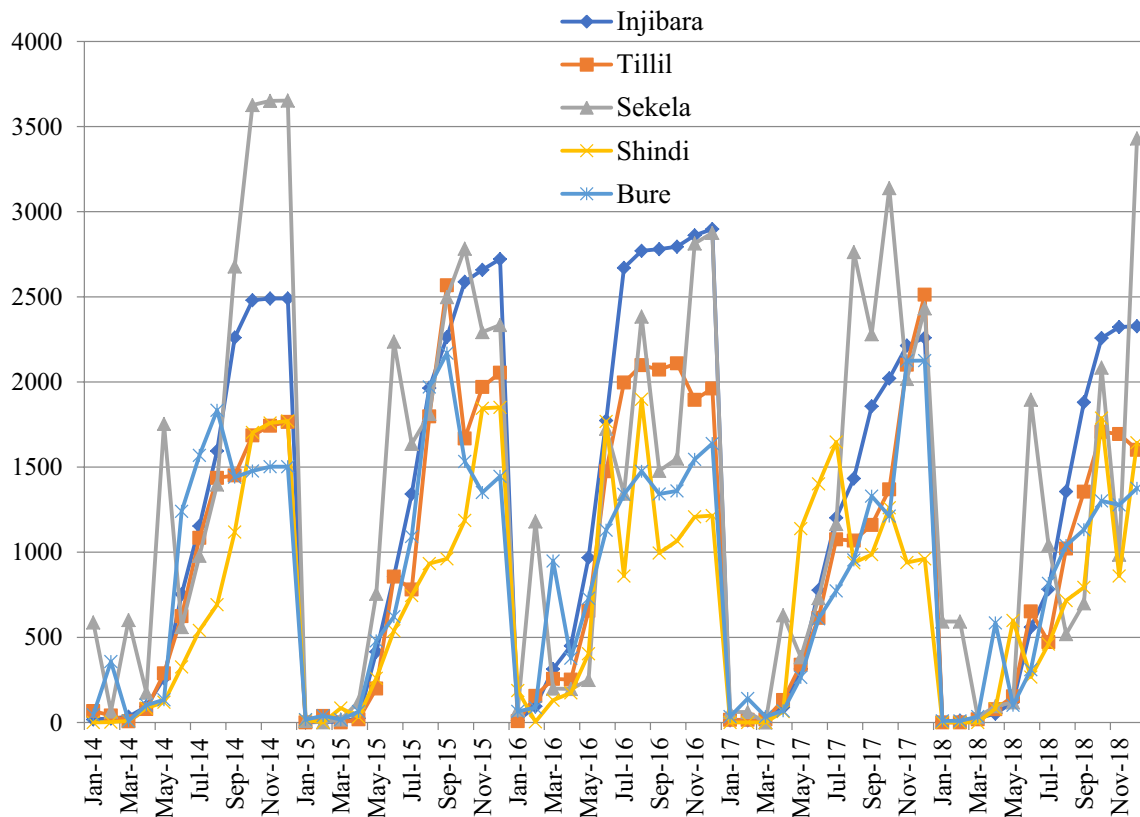


Fig. 5 Homogeneity and trend test of five rainfall station (2014–2018) years

$PX'$  represents corrected precipitation at station  $x$ ,  $PX$  represents initially recorded precipitation at station  $x$ ,  $M'$  represents the corrected slope of the double mass curve, and  $M$  represents the actual gradient of the double mass curve shown in Fig. 6.

### SWAT model set-up and simulation

#### Hydrological component of SWAT

To simulate the hydrology of a watershed, two distinct divisions were used. The first was a land stage of the

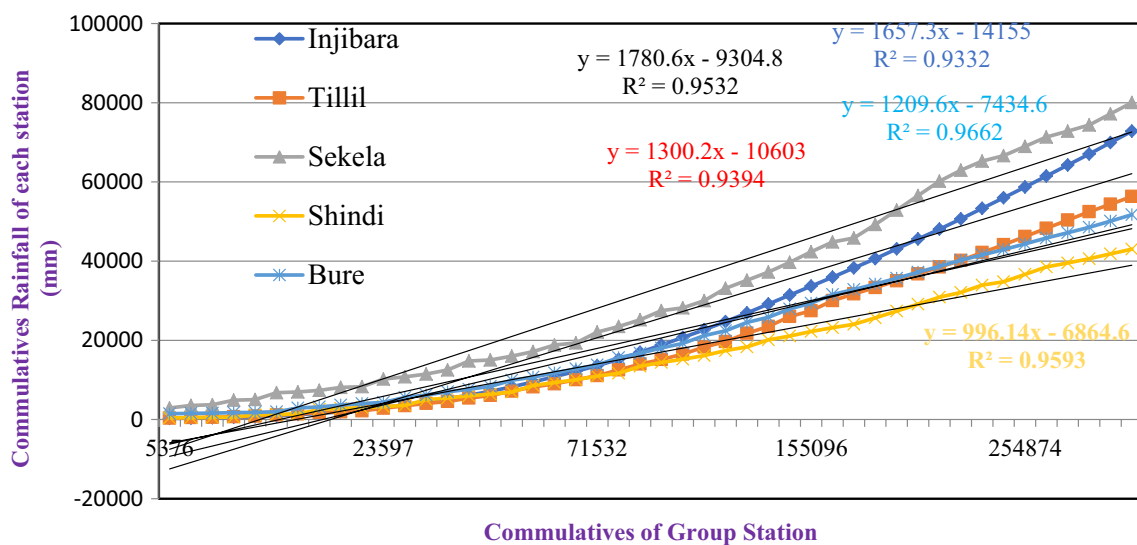


Fig. 6 Consistency checking of the five rainfall stations within and around the catchment



hydrological sequence that regulates number of nutrients, water, pesticides, and sediment loading into each sub-primary basin's channel. In the land stage of the hydrological rotation, cover evapotranspiration, storage, infiltration, surface runoff, sideways subsurface movement, redistribution, branch stations, and reoccurrence flow were all modeled. The hydrologic cycle's routing stage, defined as the transport of water, nutrients, sediments, and organic compounds through the watershed's channel network to the outflow, was the second division. In the SWAT model, the water balance equation was employed to mimic the hydrological cycle (Assfaw 2020; Saddique et al. 2020). This equation is shown below:

$$SW_t = SW_o + \sum_{(i=1)}^t (R_{\text{day}} - Q_{\text{surf}} - E_a - W_{\text{seep}} - Q_{\text{gw}}) \quad (5)$$

where  $SW_t$  is the final soil moisture at a time 't' (mm),  $SW_o$  is the initial soil moisture (mm),  $t$  is the time (days),  $R_{\text{day}}$  is the quantity of rainfall on day I (mm),  $Q_{\text{surf}}$  is the quantity of surface runoff on day I (mm),  $E_a$  is the quantity of evaporation and transpiration on day I (mm),  $W_{\text{seep}}$  is the amount of water seeping into the unsaturated zone from the surface soil on day I (mm).

The weather producer in the SWAT model can be used to simulate or measure precipitation inputs for hydrologic estimation. The delineation of watersheds and the generation of streamflow networks are the first steps in the SWAT model's modeling of the hydrological approach. The SWAT modeling format was completed in time for the first simulation, which was used to evaluate the model. Before assessing the model's performance in the catchment using the SWAT simulation results (Dibaba et al. 2020; Tena et al. 2019).

### Sensitivity analysis, calibration and validation

The sensitivity analysis was a crucial element in Arc-SWAT, as it allowed for two different types of performance studies. The first type of study classifies the impact of changing a parameter value on a simulated production quantity, such as normal streamflow, using only one modeled data. The next way of examination uses observed data to calculate the total goodness of fit between the modeled and measured time series (Welde and Gebremariam 2017). The first assessment is used to classify factors that enhance a certain model technique, while the second analysis is used to classify parameters that are influenced by the study watershed's attributes. As a consequence, vulnerability assessment is a strategy for distinguishing the greatest vulnerability characteristics that have a significant impact on the calibration and validation model, as well as defining how the model output differs throughout a range of assumed input variables (Abere et al. 2020; Alemayehu et al. 2019).

Flow simulation for 20 years of recording times is performed after a thorough preparation of the relevant input data into the Arc-SWAT model. The six-year flow data are used as a warm-up period for the simulation, which is used for the evaluation of hydrologic variables and model calibration. The simulation findings cannot be directly used for further study; instead, stream flow must be examined using evaluation, calibration, and validation models (Bufebo and Elias 2020; Tewabe and Fentahun 2020). The method of evaluating model parameters in collaboration with the model forecasted by experimental data for the same scenario was known as hydrological model calibration (Dibaba et al. 2020; Tenagashaw et al. 2022). Data from the time series of discharge at the watershed's outlet are used to calibrate and validate the SWAT model. Measured streamflow data from the years 2000 to 2005 were used to calibrate the model.

Validation is a technique for putting the calibrated model to the test using the self-determining dataset without any additional constraint modifications. The calibrated model was built in opposition to a self-governing set of measured data in order to evaluate the efficiency of future prospective administration procedures (Alemayehu et al. 2019; Yihun 2020). Validation models are based on eight years of streamflow data, covering the years 2006 to 2012.

### SWAT CUP

For SWAT alone, the SWAT CUP interface was developed. Using this universal interface, SWAT can easily be linked with any calibration or sensitivity software. The program's connection of the GLUE, Parasol, SUFI2, and MCMC procedures to SWAT is an example of this. In this investigation, sequential uncertainty fits were favored (SUFI2). Automated model calibration involves running the model, altering the unknown model parameters carefully, and then extracting the necessary outputs (corresponding to measured data) from the model output files. An interface's main function is to link a calibration program's input and output to the model.

### Model performance evaluation

To compare the model simulation of calibration and validation outputs to the experiential data, model performance estimation was necessary. A variety of strategies could be used to estimate the model performance during the calibration and validation stages. To measure the goodness-of-fit of the model method, two techniques were employed for these investigations: coefficient of determination ( $R^2$ ) and Nash–Sutcliffe Simulation Efficiency (NSE). The  $R^2$  represents how well the model explains the modification in the measured data. The determining

factor was the size of the linear relation between the simulated and experimental standards.  $R^2$  is a measure for model quality that goes from 0 to 1, with higher values suggesting lower error variance.

In contrast to the observed data variance, the NSE evaluates the normalized relative amount of remaining variation. The NSE ranges from 1.0 to  $-\infty$ , with 1.0 being the best fit. In this technique, the variance between experimental and model results is squared, and low values in time series, such as base flow or lateral subsurface flow, have a minor effect on total NSE. Furthermore, in low flow scenarios, the Nash–Sutcliffe efficiency coefficient is typically unaffected by over or under forecasting (Hassaballah et al. 2017). Within the investigation phase, this issue can be detected by cooperative forecast and experiential values.

In general, model simulations for shorter time phases are weaker than for longer time phases (Guzha 2018). The NSE statistics performance ratings listed above is for monthly time periods and must be improved for a daily time period to be appropriate in this research. Equations (6) and (7) are used to calculate the  $R^2$  and NSE values, respectively.

$$R^2 = \frac{\sum(X_i - X_{av})^2(Y_i - Y_{av})^2}{\sqrt{\sum(X_i - X_{av})^2} \sqrt{\sum(Y_i - Y_{av})^2}} \quad (6)$$

$$NSE = 1 - \frac{\sum(X_i - Y_i)^2}{\sum X_i - X_{av})^2} \quad (7)$$

where  $R^2$  represents the Model approach coefficient of determination,  $X_i$  represents the measured value ( $m^3/s$ ),  $X_{av}$  represents the average measured value ( $m^3/s$ ),  $Y_i$  represents the simulated value ( $m^3/s$ ),  $Y_{av}$  represents the average simulated value ( $m^3/s$ ), and NSE represents Nash–Sutcliffe simulation efficiency.

## Results and discussion

### Sensitive parameter

The Ribb watershed was divided into 149 HRUs and 25 sub-basins for this study. With the use of the SWAT CUP (Calibration and Uncertainty Program) model, the sensitive parameters were found (Table 1). In the Upper Ribb watershed CN2, SOL\_K, CH\_K2 SLP, and SOL\_BD were found 1st to 5th sensitive flow parameters, respectively (Table 1). On the other hand, found ESCO, SOIL-AWC, EPCO, CN2, and ALPHA\_BF as the first five subtle flow parameters. T-STAT and  $p$  values had been used to assess the parameter's level of sensitivity and significance. High absolute T-STAT values for a parameter are regarded as very sensitive, and  $p$  values near 0 as highly significant (Table 2).

### Analysis of changes in land use/cover

The simulation of LULC 2020 using the CA-Markov model was facilitated by the usage of the observed LULC 2000 and LULC 2010. The performance of the model was assessed using the kappa index by comparing the observed LULC 2020 with the simulated LULC 2020. As a result, the estimated Kappa index equals 0.85. The results suggest a powerful CA-Markov model for simulating the future LULC in the research area, as evidenced by the high level of agreement between the simulated and observed LULC in 2017. LULC is a step-by-step analysis of land cover location maps that showed five types of LULC: water body, cropland, grassland, vegetation land, and buildup area. For the years 2000, 2010, and 2020, LULC unifying classes were created. To characterize the entire LULC patterns throughout the watershed, a geographical analysis of LULC was done. The Fetam watershed includes grasslands, water bodies, vegetation, and

**Table 2** Global sensitive flow parameters

Parameter type	Parameter name	Minimum value	Maximum value	Fitted value	T-STAT value	$p$ value
HRU	R_CN2.mgt	-0.25	0.25	0.246	80.18	0
Soil	SOL-K.sol	-0.1	0.34	0.31	7.8	0
Routing	V_CH_K2.rte	125	130	126.7	-2.6	0.01
HRU	R_SLP.hru	0.05	0.1	0.052	1.98	0.048
	R_SOL_BD	0.9	1.0	0.96	-1.88	0.061
Groundwater	V_ALPHA_BF.gw	0.8	1.0	0.81	-1.513	0.131
Soil	R_SOL_AWC.sol	0.9	1.0	0.99	-1.512	0.131
Groundwater	V_GW_REVAP.gw	0.189	0.197	0.195	-1.405	0.161
HRU	V_ESCO.hru	0.125	0.163	0.13	1.269	0.205
Groundwater	V_GWQMN.gw	24.475	25	24.98	0.938	0.348
Groundwater	V_GW_DELAY.gw	448.5	449.5	449	0.923	0.357

built-up areas, as well as main components of farmed land or croplands in all parts of the watershed.

The overall coverage of cropland, vegetation, grassland, water bodies, and built-up area on the LULC map of 2000 (Fig. 7 and Table 3) was about 59.936%, 5.32%, 23.19%, 0.069%, and 11.49%, respectively, from the whole part of Fetam watershed. Due to the high population density in the Fetam watershed, this increases the amount of new settlement and farming land available. This is most likely due to deforestation actions that have occurred in the name of farming, urbanization, and rural settlement since the latter was recognized in recent years.

According to land use, land cover changes in 2010 (Fig. 8 and Table 4) showed that cropland was covered by 79.607%, followed by Grassland, Forest land, building area, and water bodies, which were covered by 15.738%, 2.62%, 1.813%, and 0.222%, respectively. Due to the expansion of farming regions from time to time, the cropland coverage was a very large area during this year.

According to the LULC map of 2020, crops covered roughly 76.918% of the overall area of the Fetam watershed (Fig. 9 and Table 5). Due to high growth of population in the Fetam watershed, this increases the amount of new settlement and farming land available. Other water bodies, vegetation, grassland, and buildup area, on the other hand, were covered to varying degrees: 0.207%, 4.082%, 15.792%, and 3.001%, respectively. This is due to the annual destruction of forests for farming and the establishment of new urban

**Table 3** Land covers areas in 2000

S. N.	TYPE	Area in hectare	Area in percent
1	Water Body	788.02	0.722
2	Vegetation	9078.60	8.318
3	Grassland	27,491.21	25.188
4	Cropland	65,416.60	59.936
5	Built-up area	6369.65	5.836
	Total	109,144.08	100

areas and rural settlements surrounding the Fetam watershed. In the Fetam watershed, cropland increased by 15% over a 20-year period, whereas vegetation land decreased by 70.02%.

Using the 2020 land use map as a baseline map, the LULC 2030 and LULC 2040 future predictions were carried out. Using LULC data between 2010 and 2020, the transition matrix and transfer probability matrix were generated.

According to the forecasted results for the period of 2020–2030, as shown in (Table 6), cropland and built-up areas are increased, while vegetation, grassland, and water bodies were decreased. Cropland, urban built-up and vegetation were expected to continue increasing from 2030 until 2040. In contrast to the outcome of the previous prediction, the rate of cropland and built-up expansion is, however, slower. Due to the farms' reliance on irrigation and the restricted amount of land available for built-up expansion,

**Fig. 7** A map of land usage and land cover in the year 2000

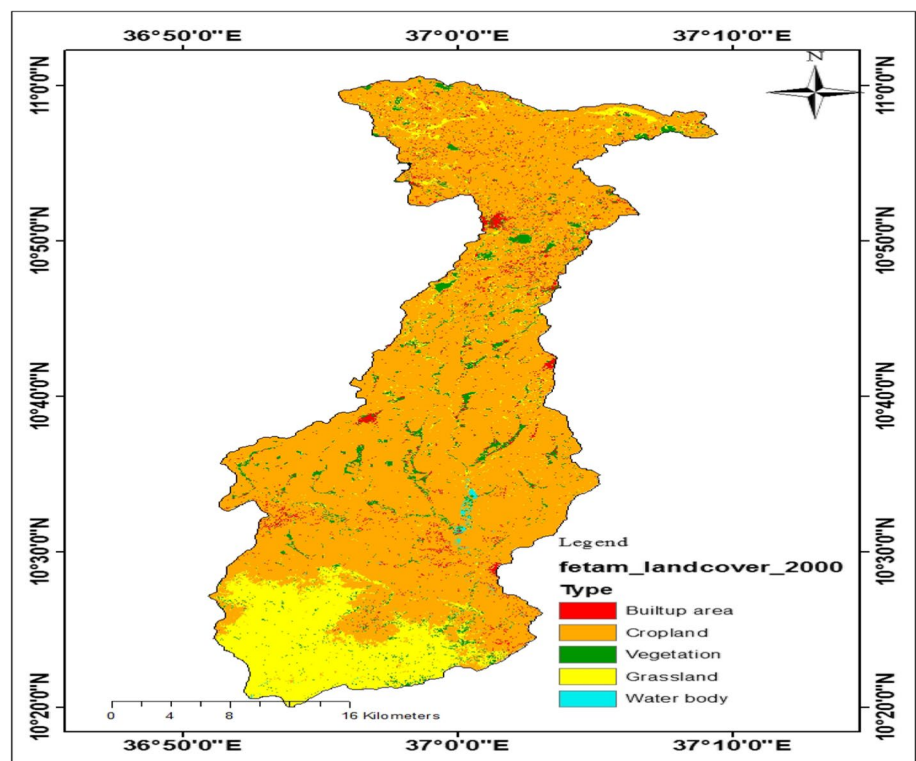


**Fig. 8** A map showing land use and land cover in 2010

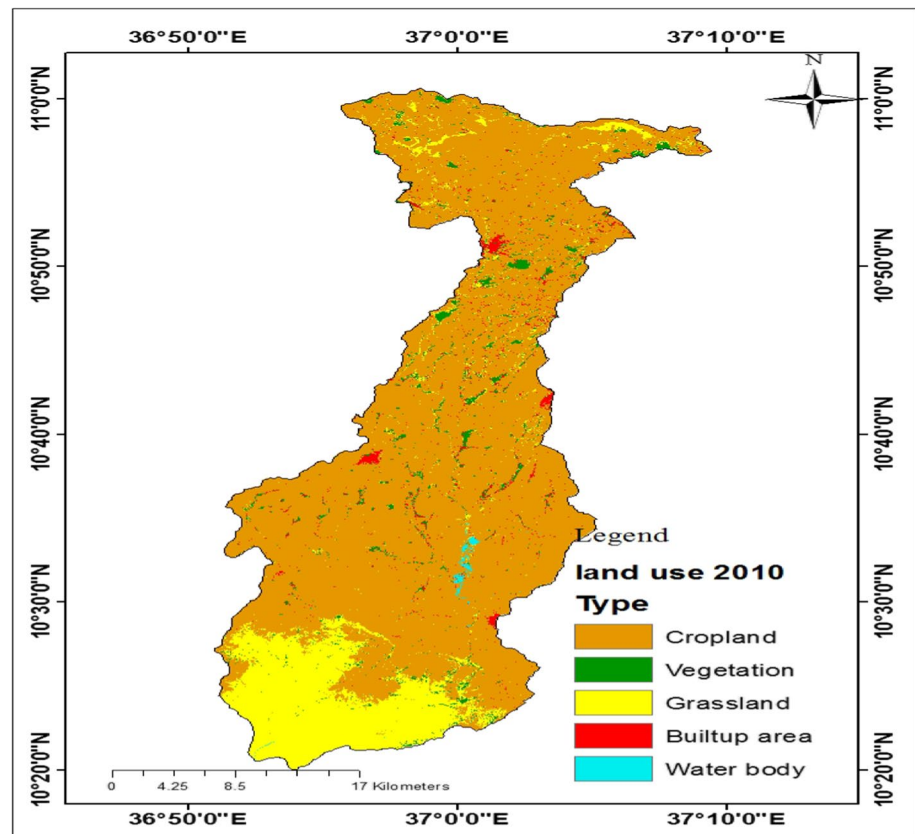


**Table 4** Land covers areas in 2010

S. N.	Type	Area in hectare	Area in percent
1	Water body	444.22	0.407
2	Vegetation	4455.26	4.082
3	Grassland	17,177.10	15.738
4	Cropland	80,337.68	73.607
5	Built-up area	6729.82	6.166
	Total	109,144.08	100

this may be feasible. Additionally, the decrease in agricultural expansions may be attributed to the extension of range land through ongoing conservation efforts (soil and water conservation efforts have already started). This might also be influenced by the rapid urbanization. Another explanation might be the expansion of the grasslands brought on by the planned afforestation.

#### Land use/cover changes detection

The ERDAS Software and GIS were used to detect land use/cover changes. Table 7 compares the detection of changes in images from 2000 to 2010, 2010 to 2020, and 2000 to 2020.

According to above table, the gradual change of LULC, particularly the incremental of cropland by percentages

of 13.671% between (2000–2010) and decreased by 3.089% between (2010–2020), and the built-up area was increased by 0.33% and 4.835% between (2000–2010) and (2010–2020), respectively, while vegetation, grassland, and water bodies were decreased by 4.236%, 9.37%, and 0.315% between (2000–2010) years and 1.462%, 0.146% and 0.138% between (2010–2020) years, respectively, the Fetam river streamflow decreased due to high percentage reductions of water body, vegetation, and grassland by 62.74%, 68.502%, and 38.097%, respectively, as well as increases in cropland and built-up area of 17.655% and 88.5024% in the watershed over 20 years.

According to Fig. 10 water bodies, vegetation and grassland were decreased for both periods of 2000–2010 and 2010–2020 and also 2000–2020 periods. However, cropland is increased and decreased during periods of 2000–2010 and 2010–2020, respectively, but increased starting from periods of 2000–2020. The buildup area was increased throughout three periods, which are 2000–2010, 2010–2020 and 2000–2020 periods.

#### Calibration and validation model of sensitive analysis

Sensitivity examination of Fetam streamflow for the sub-basins was performed using day-to-day observed and

**Fig. 9** A map of land use and land cover in 2020

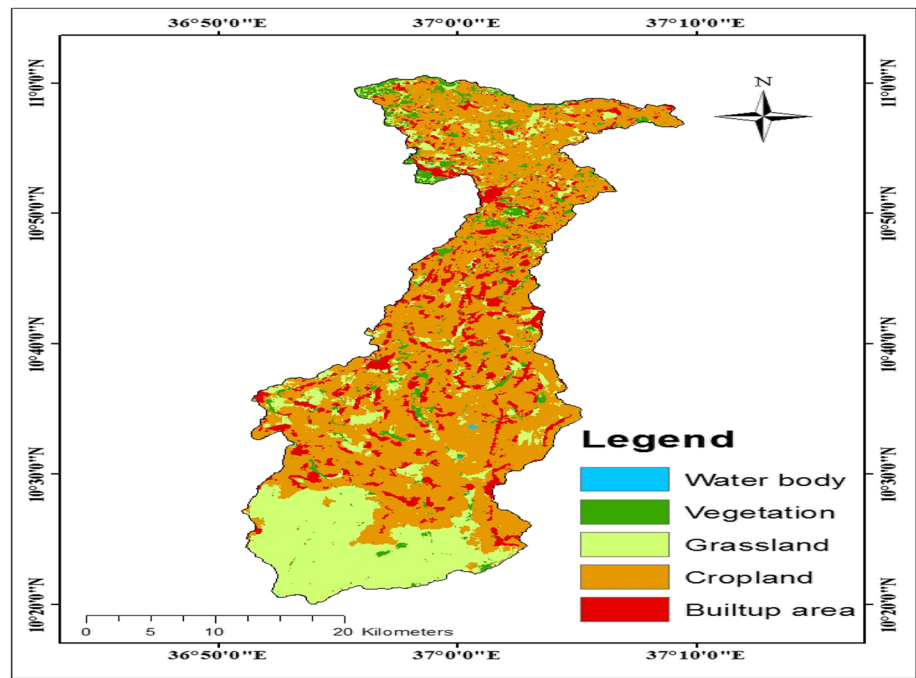


**Table 5** Land covers areas in 2020

S. N.	Type	Area in hectare	Area in percent
1	Water body	293.60	0.269
2	Vegetation	2859.57	2.62
3	Grassland	17,017.74	15.592
4	Cropland	76,966.22	70.518
5	Built-up area	12,006.94	11.001
	Total	109,144.08	100

**Table 6** Future predication of LULC of 2030 and 2040

S. N.	Type	LULC (2030)	LULC (2040)
1	Water body	0.26	0.23
2	Vegetation	2.35	2.85
3	Grassland	13.65	11.92
4	Cropland	71.85	72.3
5	Built-up area	11.89	12.7
	Total	100	100

simulated flow data to identify the most sensitive parameter and calibrate and validate the streamflow model. Any hydrologic simulation must have calibration and validation models in order to be used successfully. Using calibration and validation, this model was used to simulate Fetam streamflow. For the past 20 years, a calibration and validation model has been used. The hydrologic model was calibrated and validated by comparing observed and simulated streamflow discharge from 2000 to 2004 and 2005 to 2012, respectively.

### Model of stream flow calibration and validation

The LULC of 2000, 2010, and 2020 was calibrated for 5 years, beginning in January 2000 and ending in December 2004, and validated for 8 years, beginning in January 2005 and ending in December 2012. For the LULC of 2000, 2010, and 2020, the result of monthly streamflow between observed and stimulated values of calibrated and validated was shown to be in good agreement with a  $R^2$  and NSE.

According to Hassaballah et al. (2017), the NSE and  $R^2$  for the daily calibration and validation of the three precipitation products ranged from 0.4 to 0.80 and 0.50 to 0.80, respectively. According to Welde and Gebremariam (2017), the  $R^2$  and NSE for the monthly average streamflow values of calibration and validation are 0.88 and 0.85 and 0.85 and 0.84, respectively. Comparison of monthly average streamflow between actual and simulated values of calibration and validation models is shown in Figs. 11, 12, 13 and 14. During the calibration and validation periods, strong correlation values of 0.72–0.9 were observed and simulated, showing that the NSE and  $R^2$  Values Of The Model, Which Were accurate. However, groundwater percolation is responsible for some of the flow loss. The findings of calibrated and validated streamflow models show that simulated and observed streamflow is in good agreement. As a result of the streamflow data (Table 8), the SWAT model is a good estimate for the Fetam River streamflow (Figs. 12, 14).

**Table 7** Land use/cover changes detection from 2000–2020

Land use/cover type	Area change (hectare)	Percentage area change	Area change (hectare)	Percentage area change	Area change (hectare)	Percentage area change
	2000–2010	2000–2010	2010–2020	2010–2020	2000–2020	2000–2020
Water Body	-343.80	-0.315	-150.62	-0.138	-494.42	-0.453
Vegetation	-4573.34	-4.24	-1595.69	-1.46	-6219.03	-5.698
Grassland	-10,314.1	-9.45	-159.36	-0.146	-10,473.5	-9.596
Cropland	14,921.08	13.67	-3371.46	-3.09	11,549.6	10.582
Built-up area	360.17	0.33	5277.12	4.84	5637.25	5.165

**Fig. 10** The land use/cover change in percentage of study area

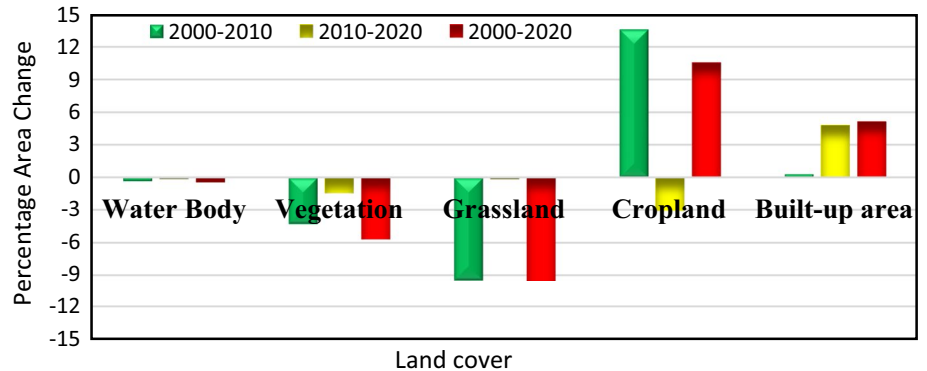


**Fig. 11** Monthly average flow between observed and simulated (2000–2004)

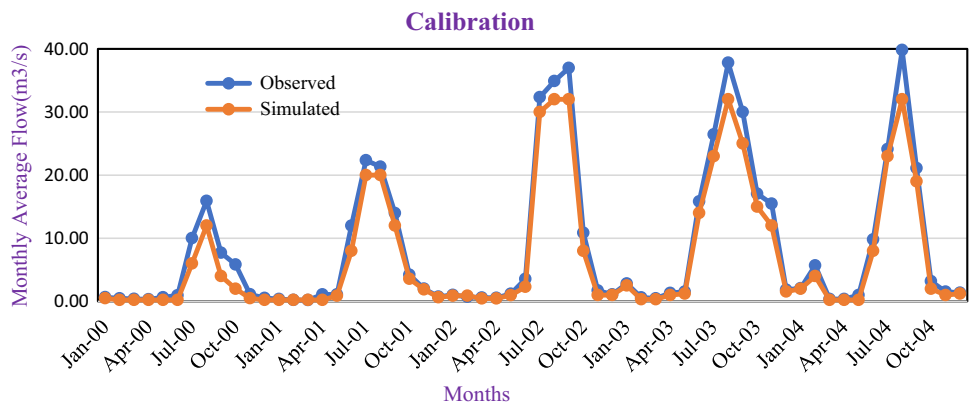


**Table 8** NSE and  $R^2$  values of Arc-SWAT estimation verses observed data

Variable	Calibration (1998–2003)		Validation (2004–2007)	
	$R^2$	NSE	$R^2$	NSE
Stream flow	0.9	0.85	0.88	0.72

**Land use/covers change impacts**

Satellite images from three separate years showed an effect on the Fetam River's streamflow, which was utilized to construct three different SWAT model simulations, according to

the findings of LULC change. The results of the simulated streamflow in the years 2000, 2010, and 2020 were not the same as the results of the whole streamflow computed to its observed streamflow. This indicates that the LULC modification had an impact on the Fetam River's monthly and seasonal streamflow.

**Assessments of the effects of changes in land use/cover on streamflow**

Land use/cover change detection of three separate years' satellite image results showed an effect on the streamflow. While calibrating and validating the model using three land use/cover maps, the simulation was run with all

**Fig. 12** Scatters plot of observed vs. simulated flow for calibration (2000–2004)

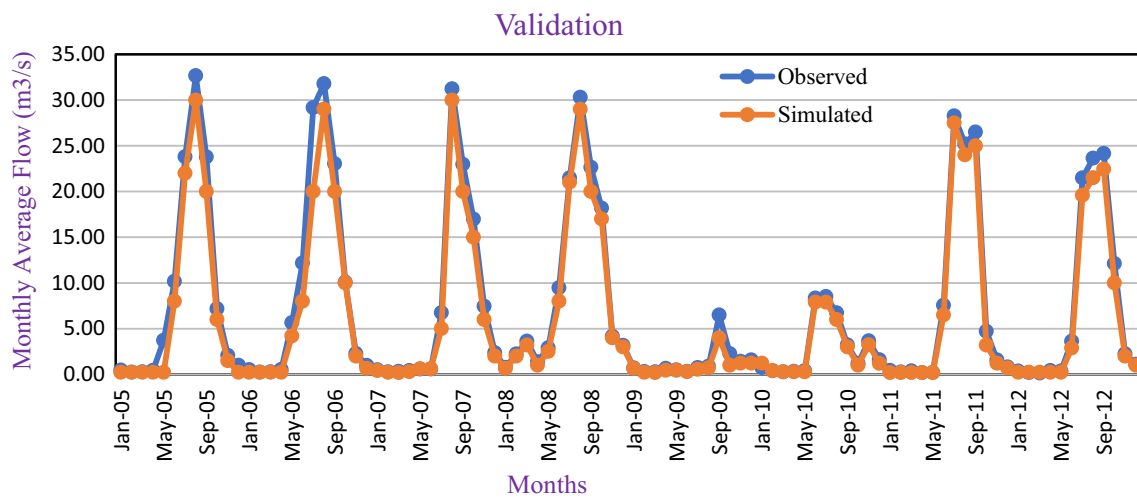
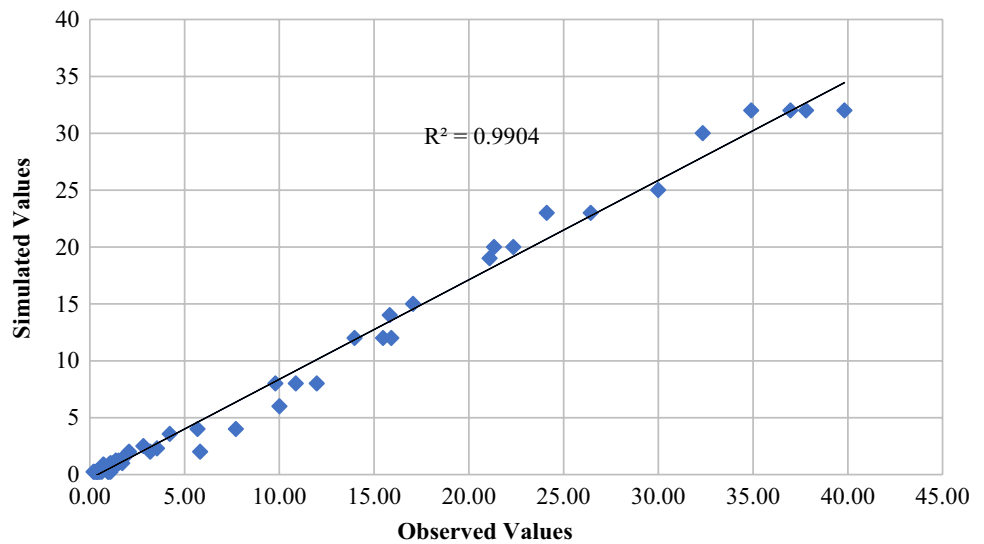


**Fig. 13** Shows the monthly average flow of observed and simulated data

other parameters measured for both simulations to quantify streamflow variability and observe how land use/cover change affected it. According to Jemberie et al. (2016), the mean monthly stream flow was increased by 29.44 m<sup>3</sup>/s for wet season and decreased by 4.44 m<sup>3</sup>/s in dry season over 25 years period. Therefore, the Fetam River watershed's monthly average streamflow decreased from 2000 to 2010, and 2010 to 2020, by 2.885 m<sup>3</sup>/s and 6.33 m<sup>3</sup>/s, respectively.

Due to increased agricultural and other land use/cover change, seasonal streamflow in the Fetam watershed decreases in the dry period compared to the wet period, resulting in higher flow during the wet periods. The results of this study indicated that the seasonal streamflow decreased by 5.54 m<sup>3</sup>/s, and 0.38 m<sup>3</sup>/s and 0.23 m<sup>3</sup>/s and 12.28 m<sup>3</sup>/s, respectively, at 2000–2010 and 2010–2020 during the dry and rainy seasons. LULC variations of simulated

mean monthly streamflow of Fetam watershed during study periods were presented in 2000, 2010, and 2020 (Fig. 15). For both the calibration and validation phases of land use/cover, these results showed a relatively increased streamflow from 2000 to 2020.

Changes in land use/cover have an effect on the Fetam River's average monthly and seasonal streamflow throughout the year, as shown below (Table 9).

### Impacts of LULC change on groundwater and surface runoff

There are two LULC change scenarios, the first for LULCC from 2020 to 2030 and the second for LULCC from 2020 to 2040 scenarios with the base land use map of 2020, were used to evaluate the hydrological responses of the watershed

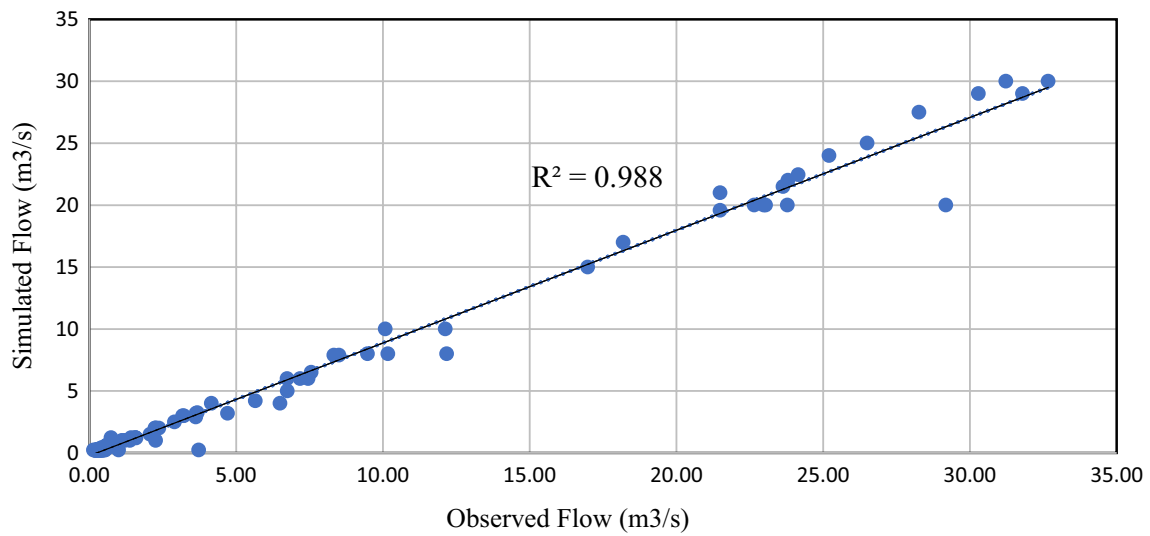


**Fig. 14** Validation scatter plot of observed vs. simulated flow (2005–2012)

**Fig. 15** Mean monthly flow contrast **a** calibration and **b** validation years

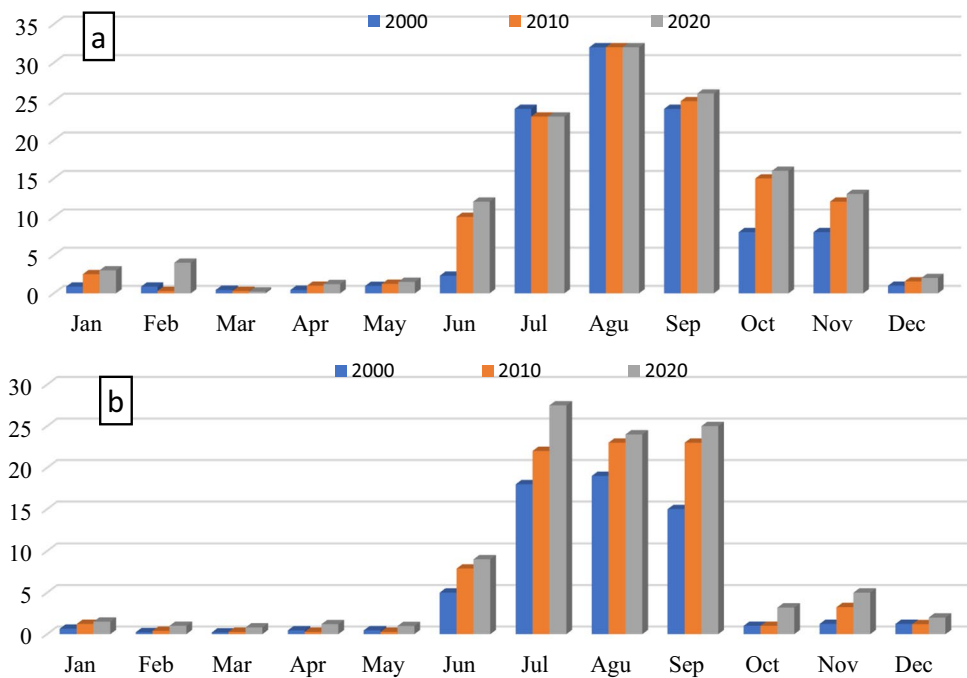


**Table 9** LULC change impact on average monthly and seasonal stream flow

Year		2000	2010	2020	Change (2000–2010)	Change (2010–2020)	
Stream flow (m <sup>3</sup> /s)	Average monthly	33.945	31.06	24.73	–2.885	–6.33	
	Seasonal	Dry	6.63	1.09	0.71	–5.54	–0.38
		Wet	61.26	61.03	48.75	–0.23	–12.28



to LULC change. Changes in land use/cover had an impact on components of streamflow in the Fetam watershed due to the effects of groundwater discharges and surface runoff throughout the year. The watershed's hydrological responses were taken into account in terms of the processes affecting yearly surface runoff; annual groundwater, total water yield, and potential evapotranspiration were shown in (Table 10). The mean annual surface water runoff and total water yield will rise as a result of the significant anticipated changes in land use between 2020 and 2030 and 2020 to 2040, whereas groundwater recharge and potential evapotranspiration will fall. However, the frequency of LULC changes was correlated with the rates of rise and fall. For instance, it was expected that the first scenario would have a higher rate of agricultural development and a lower rate of forest decrease. As a result, compared to the baseline scenario, the rate of increase in surface flow was slower, rising from 2030 to 2040.

In the first and second scenarios, the surface runoff and water yield were increased by 6.85% and 2.05% and 8.15% and 2.85%, respectively. In the first and second scenarios, the groundwater level and potential evapotranspiration were decreased by 1.5% and 1.45% and 0.85% and 1.76%, respectively. Due to the higher decrease in forest and shrub land, the declining rate is larger for the changes from 2020 to 2030. This is a good example of how changing the land cover can affect groundwater management; for example, if the amount of shrub land grows, groundwater recharge will also increase. Evapotranspiration decreased as a result of the loss of forestland, which caused evapotranspiration to diminish. Furthermore, a lack of soil moisture brought on by increasing runoff may also be a factor in the drop in evapotranspiration. A related study found that as a result of less rainfall, PET decreases when soil moisture is low (Tenagashaw et al. 2022; Woldeesenbet et al. 2018).

With the greatest growth of agricultural areas, urban expansion, and decline of forested and shrub land, there is a corresponding greatest increase in surface flow and greatest decrease in groundwater recharge. This shows that converting large areas of LULC to intensive agriculture and settlements will decrease the soil's ability to absorb water, resulting in a significant increase in surface runoff. Groundwater flow declines as a result of decreased soil water infiltration. Additionally, the growing population's increased need for

groundwater consumption could worsen the groundwater crisis by increasing groundwater withdrawal. According to recent research by Dibaba et al. (2020) in the Finchaa catchment, the high variations in LULC caused the catchment's springs to run dry and the volume of water to decrease. As a result, flow discharges during the dry season were lower than base flow, while flow discharge during the rainy months was higher than base flow. Changes in land use/cover had a significant impact on runoff output, infiltration rate, and soil water-holding capacity in watersheds, according to this study finding.

## Conclusions

This study focuses on the effects of land use/cover change and future prediction of LULC change on streamflow of the Fetam watershed by using Cellular Automata (CA)-Markov in IDRISI software. There are five major parameters were identified for this study of LULC changes, and these are water bodies, vegetation, grassland, cropland, and built-up area. The results of this study indicated that the cropland and built-up area were increased by 15% and 46.95%, respectively, over a 20-years period (2000–2020); however, water bodies, vegetative land, and grassland decreased by 62.74%, 70.02%, and 38.1%, respectively. The results of this study indicated that the future forecasted results of cropland and built-up areas are increased, while vegetation, grassland, and water bodies were decreased for the period of 2020–2030 and 2030–2040. The major causes of this LULC changes are rapid population growths around watersheds, as well as pressures to expand farming land and develop urbanization areas. Performances evaluation of calibration and validation of streamflow were showed good agreement between observed and simulated values of NSE and  $R^2$ , which are 88% and 72% and 90% and 85%, respectively. This study showed that monthly average streamflow decreased from 2000 to 2010, and 2010 to 2020, by 2.885 m<sup>3</sup>/s and 6.33 m<sup>3</sup>/s, respectively. The results of this study indicated that the seasonal streamflow decreased by 5.54 m<sup>3</sup>/s, and 0.38 m<sup>3</sup>/s and 0.23 m<sup>3</sup>/s and 12.28 m<sup>3</sup>/s, respectively, at 2000–2010 and 2010–2020 during the dry and rainy seasons. Impacts of LULC changes in the first and second scenarios, the surface runoff and water yield were increased by 6.85% and 2.05% and 8.15% and 2.85%, respectively. But the groundwater level and potential evapotranspiration were decreased by 1.5% and 1.45% and 0.85% and 1.76%, respectively. Due to high amounts of sediment loads and surface runoff during the rainy season, as well as deforestation and increased cultivated land. Therefore, the effect of land use/cover change on streamflow is a critical issue that affects volumes of streamflow discharges year to year. In general, the impacts of land use/cover change on streamflow are significant considerations for planning and

**Table 10** Variation in the components of the yearly water balance under LULC changes

Land use	Surface runoff (%)	Groundwater (%)	Water yield (%)	PET (%)
2030	6.85	−1.5	2.05	−1.45
2040	8.15	−0.85	2.85	−1.76

implementing water resource projects. In order to address the risks, effective land-use planning and climate-resilient water management strategies will be improved.

**Funding** There are no funds, grants, or other supports that were received during the preparation of this manuscript and to publish.

**Accessibility of data and materials** This article contains all of the data that were collected and evaluated during the study.

## Declarations

**Conflict of interest** There is no conflict of interest for this publication; as corresponding authors, I confirm that the manuscript has been read and approved for submission by all the names of authors.

**Open Access** This article is licensed under a Creative Commons Attribution 4.0 International License, which permits use, sharing, adaptation, distribution and reproduction in any medium or format, as long as you give appropriate credit to the original author(s) and the source, provide a link to the Creative Commons licence, and indicate if changes were made. The images or other third party material in this article are included in the article's Creative Commons licence, unless indicated otherwise in a credit line to the material. If material is not included in the article's Creative Commons licence and your intended use is not permitted by statutory regulation or exceeds the permitted use, you will need to obtain permission directly from the copyright holder. To view a copy of this licence, visit <http://creativecommons.org/licenses/by/4.0/>.

## References

- Abere T, Adgo E, Afework S (2020) Trends of land use/cover change in Kecha-Laguna paired micro watersheds, Northwestern Ethiopia. *Cogent Environ Sci* 6(1):1801219
- Abidin RZ, Sulaiman MS, Yusoff N (2017) Erosion risk assessment: a case study of the Langat Riverbank in Malaysia. *Int Soil Water Conserv Res* 5:26–35
- Alemayehu F, Tolera M, Tesfaye G (2019) Land use land cover change trend and its drivers in somodo watershed Southwestern, Ethiopia. *Afr J Agric Res* 14(2):102–117
- Alemu AM, Seleshi Y, Meshesha TW (2022) Modeling the spatial and temporal availability of water resources potential over Abbay river basin, Ethiopia. *J Hydrol Reg Stud* 44:101280
- Anmut EK, Tesfu AT, Negash WA (2020) Evaluation of stream flow under land use land cover change: a case study of Chemoga Catchment, Abay Basin, Ethiopia. *Afr J Environ Sci Technol* 14(1):26–39. <https://doi.org/10.5897/ajest2019.2759>
- Assfaw AT (2020) Modeling impact of land use dynamics on hydrology and sedimentation of Megech Dam Watershed, Ethiopia. *Sci World J* 1–20
- Bekele T (2019) Effect of land use and land cover changes on soil erosion in Ethiopia. *Int J Agric Sci Food Technol* 5:26–34. <https://doi.org/10.17352/2455-815x.000038>
- Bogale A (2020) Review, impact of land use/cover change on soil erosion in the Lake Tana Basin, Upper Blue Nile, Ethiopia. *Appl Water Sci*. <https://doi.org/10.1007/s13201-020-01325-w>
- Bufebo B, Elias E (2020) Effects of land use/land cover changes on selected soil physical and chemical properties in shenkolla watershed, South Central Ethiopia. *Adv Agric* 2020:1–8. <https://doi.org/10.1155/2020/5145483>
- Chang Y, Hou K, Li X, Zhang Y, Chen P (2018) Review of land use and land cover change research progress. In: IOP Conference Series: Earth and Environmental Science, vol 113. IOP Publishing, p 012087
- Chen H, Fleskens L, Baartman J, Wang F, Moolenaar S, Ritsema C (2020) Impacts of land use change and climatic effects on streamflow in the Chinese Loess Plateau: a meta-analysis. *Sci Total Environ* 703:134989. <https://doi.org/10.1016/j.scitotenv.2019.134989>
- Chimdessa Ejeta K, Kebede D, Alamirew D (2019) Analysis of climate and land use/land cover changes and their impacts on river discharge and soil loss in the Didedissa river basin, South West Blue Nile, Ethiopia (Doctoral Dissertation, Haramaya University)
- Dibaba WT, Demissie TA, Miegel K (2020) Watershed hydrological response to combined land use/land cover and climate change in highland ethiopia: Finchaa catchment. *Water (switzerland)* 12(6):1801. <https://doi.org/10.3390/w12061801>
- Disse M, Fenta Mekonnen D, Duan Z, Rientjes T (2018) Analysis of the combined and single effects of LULC and climate change on the streamflow of the Upper Blue Nile River Basin (UBNRB): using statistical trend tests, remote sensing landcover maps and the SWAT model. In: EGU general assembly conference abstracts, 2018, April
- Fentie SF, Jembere K, Fekadu E, Wasie D (2020) Land use and land cover dynamics and properties of soils under different land uses in the tejibara watershed, Ethiopia. *Sci World J* 1–12
- Gashaw T, Tulu T, Argaw M, Worqlul AW (2018) Modeling the hydrological impacts of land use/land cover changes in the Andassa watershed, Blue Nile Basin, Ethiopia. *Sci Total Environ* 619:1394–1408
- Gashaw T, Worqlul AW, Dile YT, Addisu S, Bantider A, Zeleke G (2020) Evaluating potential impacts of land management practices on soil erosion in the Gilgel Abay watershed, upper Blue Nile basin. *Heliyon* 6(8):e04777. <https://doi.org/10.1016/j.heliyon.2020.e04777>
- Guzha AC, Rufino MC, Okoth S, Jacobs S, Nóbrega RLB (2018) Impacts of land use and land cover change on surface runoff, discharge and low flows: evidence from East Africa. *J Hydrol Reg Stud* 15:49–67
- Hasan S, Shi W, Zhu X (2020) Impact of land use land cover changes on ecosystem service value—a case study of Guangdong, Hong Kong, and Macao in South China. *PLoS ONE* 15(4):1–20. <https://doi.org/10.1371/journal.pone.0231259>
- Hassaballah K, Mohamed Y, Uhlenbrook S, Biro K (2017) Analysis of streamflow response to land use and land cover changes using satellite data and hydrological modelling: case study of Dinder and Rahad tributaries of the Blue Nile (Ethiopia-Sudan). *Hydrol Earth Syst Sci* 21(10):5217–5242. <https://doi.org/10.5194/hess-21-5217-2017>
- Hu Y, Zhu Z, Xiao J, Shao H, Zhao L, Xu M, Zhuang J (2019) Atomic scale study of stress-induced misaligned subsurface layers in KDP crystals. *Sci Rep* 9(1):1–9
- Hyandyeb CB, Worqul A, Martz LW, Muzuka AN (2018) The impact of future climate and land use/cover change on water resources in the Ndembera watershed and their mitigation and adaptation strategies. *Environ Syst Res* 7(1):1–24
- Jemberie M (2016) Evaluation of land use land cover change on stream flow: a case study Ofdedissa Sub Basin. *Int J Innov Eng Res Technol* 3(8):44–60
- Kidane M, Bezie A, Kesete N, Tolessa T (2019) The impact of land use and land cover (LULC) dynamics on soil erosion and sediment yield in Ethiopia. *Heliyon* 5(12):e02981. <https://doi.org/10.1016/j.heliyon.2019.e02981>
- Mekonnen YA, Mengistu TD, Asitatie AN, Kumilachew YW (2022) Evaluation of reservoir sedimentation using bathymetry survey: a case study on Adebra night storage reservoir. *Ethiopia Appl Water Sci* 12(12):269
- Moges MA, Schmitter P, Tilahun SA, Ayana EK, Ketema AA, Nigussie TE, Steenhuis TS (2017) Water quality assessment by measuring and using landsat 7 ETM+ images for the current and previous trend perspective: lake. *JWARP* 09:1564–1585. <https://doi.org/10.4236/jwarp.2017.912099>

- Owar Othow O, Legesse Gebre S, Obsi Gemedo D (2017) Analyzing the rate of land use and land cover change and determining the causes of forest cover change in Gog District, Gambella Regional State, Ethiopia. *J Remote Sens GIS* 06(04):12–13. <https://doi.org/10.4172/2469-4134.1000219>
- Pan S, Liu D, Wang Z, Zhao Q, Zou H, Hou Y, Liu P, Xiong L (2017) Runoff responses to climate and land use/cover changes under future scenarios. *Water* 9(7):475
- Roy A, Inamdar AB (2019) Multi-temporal land use land cover (LULC) change analysis of arid semi-arid river basin in western India following a robust multi-sensor satellite image calibration strategy. *Heliyon* 5(4):e01478
- Saddique N, Mahmood T, Bernhofer C (2020) Quantifying the impacts of land use/land cover change on the water balance in the afforested River Basin, Pakistan. *Environ Earth Sci* 79(19):1–13. <https://doi.org/10.1007/s12665-020-09206-w>
- Tena TM, Mwaanga P, Nguvulu A (2019) Impact of land use/land cover change on hydrological components in Chongwe River Catchment. *Sustainability (switzerland)* 11(22):6415. <https://doi.org/10.3390/su11226415>
- Tenagashaw DY, Muluneh M, Metaferia G, Mekonnen YA (2022) Land use and climate change impacts on streamflow using SWAT model, Middle Awash Sub Basin, Ethiopia. *Water Conserv Sci Eng* 7(3):183–196
- Tewabe D, Fentahun T (2020) Assessing land use and land cover change detection using remote sensing in the Lake Tana Basin, Northwest Ethiopia. *Cogent Environ Sci* 6(1):1778998
- Welde K, Gebremariam B (2017) Effect of land use land cover dynamics on hydrological response of watershed: case study of Tekeze Dam watershed, northern Ethiopia. *Int Soil Water Conserv Res* 5(1):1–16
- Woldesenbet TA, Elagib NA, Ribbe L, Heinrich J (2018) Catchment response to climate and land use changes in the Upper Blue Nile sub-basins, Ethiopia. *Sci Total Environ* 644:193–206
- Yang C, Wu G, Chen J, Li Q, Ding K, Wang G, Zhang C (2019) Simulating and forecasting spatio-temporal characteristic of land-use/cover change with numerical model and remote sensing: a case study in Fuxian Lake Basin, China. *Eur J Remote Sens* 52(1):374–384
- Yihun (2020) Impact of land use and land cover change on stream flow and sediment yield, a case of Jedeb And Chemoga Watershed, Upper Blue Nile Basin, Ethiopia. <http://dspace.org/http/hdl.handle.net/123456789/11040>
- Yohannes H, Soromessa T (2018) Land suitability assessment for major crops by using GIS-based multi-criteria approach in Andit Tid watershed, Ethiopia. *Cogent Food Agric* 4(1):1470481

**Publisher's Note** Springer Nature remains neutral with regard to jurisdictional claims in published maps and institutional affiliations.